LAWRENCE
LIVERMORE
NATIONAL
LABORATORY

LLNL-TR-461511

NOx Sensor Development

L. Y. Woo, R. S. Glass

November 2, 2010

Disclaimer

This work performed under the auspices of the U.S. Department of Energy by Lawrence Livermore National Laboratory under Contract DE-AC52-07NA27344.

Agreement 8697 - NO_x Sensor Development

Leta Y. Woo and Robert S. Glass
Lawrence Livermore National Laboratory
P.O. Box 808, L-103
Livermore, CA 94551-9900
(925) 423-7140; fax: (925) (422-5844); e-mail: glass3@llnl.gov

DOE Technology Manager: Jerry L. Gibbs
(202) 586-1182; fax: (202) 586-1600; e-mail: jerry.gibbs@ee.doe.gov

Contractor: Lawrence Livermore National Laboratory, Livermore, California
Prime Contract No.: W-7405-Eng-48; LLNL-TR-418835

Objectives

- Develop an inexpensive, rapid-response, high-sensitivity and selective electrochemical sensor for oxides of nitrogen (NO_x) for compression-ignition, direct-injection (CIDI) exhaust gas monitoring
- Explore and characterize novel, effective sensing methodologies based on impedance measurements and designs and manufacturing methods that could be compatible with mass fabrication
- Collaborate with industry in order to (ultimately) transfer the technology to a supplier for commercialization

Approach

- Use an ionic (O^{2-}) conducting ceramic as a solid electrolyte and metal or metal-oxide electrodes
- Correlate NO_x concentration with changes in impedance by measuring the cell response to an ac signal
- Evaluate sensing mechanisms and aging effects on long-term performance using electrochemical techniques
- Collaborate with Ford Research Center to optimize sensor performance and perform dynamometer testing

Accomplishments

- Modified sensor designs to successfully improve mechanical robustness for withstanding engine vibrations and prevent failure during engine/vehicle dynamometer testing
- Developed a preliminary strategy to mitigate major noise factors and improve accuracy by quantifying effects of temperature, water, and oxygen to generate a numerical algorithm
- Publications/Presentations:
  - L.Y. Woo, et al. "Effect of electrode material and design on sensitivity and selectivity for high temperature impedancemetric NO_x sensors." *J. Electrochem. Soc.*, 157(3):J81-87, 2010
  - Oral presentations at the American Ceramic Society 34th International Conference and Exposition on Advanced Ceramics and Composites; the 217th Electrochemical Society Meeting; and the 2010 DOE Vehicle Technologies and Hydrogen Programs Annual Merit Review and Peer Evaluation Meeting

Future Directions

- Continue developing more advanced prototypes suitable for cost-effective, mass manufacturing
- Continue evaluating performance of prototypes, including long-term stability and cross-sensitivity, in laboratory, dynamometer, and on-vehicle tests
- Continue efforts to initiate the technology transfer process to a commercial entity

Introduction

NO_x compounds, specifically NO and NO_2, are pollutants and potent greenhouse gases. Compact and inexpensive NO_x sensors are necessary in the next generation of diesel (CIDI) automobiles to meet government emission requirements and enable the more rapid introduction of more efficient, higher fuel economy CIDI vehicles.[1-3]

Because the need for a NO_x sensor is recent and the performance requirements are extremely challenging, most are still in the development phase.[4-6] Currently, there is only one type of NO_x sensor that is sold commercially, and it seems unlikely to meet more stringent future emission requirements.

Automotive exhaust sensor development has focused on solid-state electrochemical technology, which has proven to be robust for in-situ operation in harsh, high-temperature environments (e.g., the oxygen stoichiometric sensor). Solid-state sensors typically rely on yttria-stabilized zirconia (YSZ) as the oxygen-ion conducting electrolyte and then target different types of metal or metal-oxide electrodes to optimize the response.[2-6]

Electrochemical sensors can be operated in different modes, including amperometric (a current is measured) and potentiometric (a voltage is measured), both of which employ direct current (dc) measurements. Amperometric operation is costly due to the electronics necessary to measure the small sensor signal (nanoampere current at ppm NO_x levels), and cannot be easily improved to meet the future technical performance requirements. Potentiometric operation has not demonstrated enough promise in meeting long-term stability requirements, where the voltage signal drift is thought to be due to aging effects associated with electrically driven changes, both morphological and compositional, in the sensor.[7]

Our approach involves impedancemetric operation, which uses alternating current (ac) measurements at a specified frequency. The approach is described in detail in previous reports and several publications (See Ref. 8-11). Briefly, impedancemetric operation has shown the potential to overcome the drawbacks of other approaches, including higher sensitivity towards NO_x, better long-term stability, potential for subtracting out background interferences, total NO_x measurement, and lower cost materials and operation.[8-11]

Past LLNL research and development efforts have focused on characterizing different sensor materials and understanding complex sensing mechanisms.[8-11] Continued effort has led to improved prototypes with better performance, including increased sensitivity (to less than 5 ppm) and long-term stability, with more appropriate designs for mass fabrication, including incorporation of an alumina substrate with an imbedded heater.

Efforts in the last year to further improve sensor robustness have led to successful engine dynamometer testing with prototypes mounted directly in the engine manifold. Previous attempts had required exhaust gases to be routed into a separate furnace for testing due to mechanical failure of the sensor from engine vibrations. A more extensive cross-sensitivity study was also undertaken this last year to examine major noise factors including fluctuations in water, oxygen, and temperature. The quantitative data were then used to develop a strategy using numerical algorithms to improve sensor accuracy.

The ultimate goal is the transfer of this technology to a supplier for commercialization. Due to the recent economic downturn, suppliers are demanding more comprehensive data and increased performance analysis before committing their resources to take the technology to market. Therefore, our NO_x sensor work requires a level of technology development more thorough and extensive than ever before.

Background

For an electrochemical cell with two electrodes, impedancemetric sensing requires that at least one of the electrodes act as the "sensing" electrode with preferable response to NO_x over other gas phase components. This contrasts to the case in potentiometric sensing, which relies on differential measurements between the two electrodes. Therefore, the impedancemetric sensor design is more flexible and can either contain one sensing electrode and one counter (i.e., non-sensing) electrode, or two sensing electrodes. It opens up the opportunity to use a greater variety of materials.

Both electrode composition and microstructure influence sensitivity, which relies on limiting the oxygen reaction on the electrode so that the NO_x reaction can be resolved.[9-11] Impedancemetric sensing is possible with a variety of electrode materials, both metal and metal oxides, that meet general sensor criteria, which include a dense microstructure and appropriate composition to limit the catalytic activity towards oxygen.[10-11]

Impedance is defined as the measured response to an alternating current and is a complex quantity with both magnitude and phase angle information. The phase angle has been found to provide a more stable response at higher operating frequencies and is chosen as the sensor signal.[8-11]

In previous work, impedancemetric sensing of either gold or strontium-doped lanthanum manganite (LSM), an electronically conducting metal oxide, electrodes was investigated in laboratory and engine testing. Preliminary results indicated that gold electrodes have good stability and the potential for low water cross-sensitivity, but also have a higher thermal expansion coefficient and lower melting temperature than the YSZ electrolyte, which limit processing flexibility. LSM electrodes have high melting temperatures and better thermal expansion match with YSZ, but have shown more water cross-sensitivity than gold.

Previous work also evaluated more advanced prototypes incorporating alumina substrates with imbedded heaters, provided by Ford Motor Company. Figure 1a shows the substrate with the sensor located at one end with leads located on the opposite end designed for packaging into a protective sensor housing (Fig. 1b) suitable for directly mounting into the exhaust manifold.

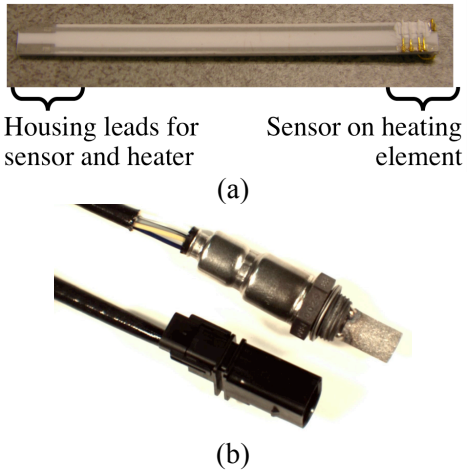

Figure 1. Picture of (a) alumina substrate with imbedded heater, provided by Ford Motor Company, suitable for packaging into (b) protective sensor housing.

Experimental

Two different sensing materials, Au and LSM, were investigated. Figure 2a shows a schematic of a prototype using Au wire as the sensing electrode and alumina with an imbedded Pt resistive heater as the substrate (70 mm × 4 mm × 1 mm, see Fig. 1a). The substrate has a total of four leads, two leads for the Pt resistive heater located on one side, and two leads for the sensor located on the opposite side.

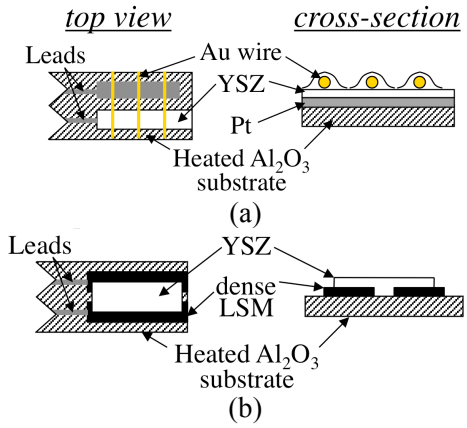

Figure 2. Schematic of NO_x prototype sensors using either (a) Au wire or (b) dense LSM as the sensing electrode.

One of the substrate leads contacted the Pt counter electrode. Yttria-stabilized zirconia (YSZ, 8 mol% yttria doping) slurry was then applied on top of the Pt. Au wires were then added and additional YSZ slurry was applied on top of the wires with the entire assembly fired at 1000°C to produce the porous YSZ electrolyte. The second substrate lead for the sensor housing contacted the Au wire.

Figure 2b shows a schematic of the prototype using LSM as the sensing electrode. A dense pellet was prepared with commercial $(La_{0.85}Sr_{0.15})_{0.98}Mn$ oxide powder (Praxair) by pressing in a uniaxial die and sintering at 1250°C. Two pieces of LSM (6 mm × 2 mm × 1 mm) were machined and attached to the top of the substrate using Pt paste and fired to 1200°C. YSZ slurry was applied on top of the dense LSM pieces and the assembly fired at 1000°C.

Heater voltage was set between 9-9.5 V, which corresponded to approximately 600 to 650°C. The exact temperature corresponding to the heater voltage was not known, but was correlated with the behavior of similar prototypes that underwent furnace testing. Future prototypes may incorporate resistive temperature detectors to more accurately determine temperature.

A more extensive laboratory study of the Au wire prototype was performed using an alumina substrate (10 mm × 10 mm × 0.5 mm) without imbedded heaters. The alternative substrate was more suitable for controlled temperature testing in a tube

furnace. The sensor geometry was similar to that shown in Fig. 2a.

Gas composition was controlled in laboratory testing by mixing air, N_2, NO, and ammonia (NH_3) using a standard gas handling system equipped with thermal mass flow controllers. Humidity was controlled using a water injection system monitored with a humidity sensor.

Dynamometer testing of real diesel exhaust was performed at Ford Research Center using an engine test cell fitted with a urea-based selective catalytic reduction (SCR) system for reducing NO_x emissions. The exhaust gas composition was analyzed with Fourier Transform Infrared (FTIR) spectroscopy. The test setup also included a commercially available NO_x sensor located alongside the prototype. Electrochemical measurements were performed using a Solartron 1260 Impedance Analyzer where the phase angle response at 5 Hz and 100 mV excitation amplitude was chosen as the sensor signal.

Results and Discussion

Engine dynamometer testing

Previous prototype designs lacked the necessary mechanical robustness for mounting directly to the exhaust manifold during engine dynamometer testing. Instead, exhaust gases had to be routed into a separate test setup. Real engine conditions, including vibrations, caused either the Au wire or dense LSM to detach from the substrate. To improve adhesion, an additional ceramic adhesive was used to anchor the Au wire and dense LSM to the substrate.

Testing was performed on a laboratory test stand at Ford Motor Company both prior to and after the prototypes being directly mounted into the exhaust manifold and operated for several hours under real-world engine conditions. Figure 3 shows results for the Au wire and LSM prototypes on the Ford laboratory test stand in 4% O_2 and 4% H_2O with 30 sec. pulses of 20 ppm NO.

The results in Fig. 3 show reproducible responses before and after several hours of diesel engine dynamometer testing. The higher sensitivity of the Au wire prototype compared to the LSM can be explained by previous results indicating that LSM has larger oxygen catalytic activity and therefore lower sensitivity when operated at similar temperatures as the Au wire prototype.[11] The modification of sensor prototypes with the addition of the ceramic adhesive successfully improved mechanical stability and robustness.

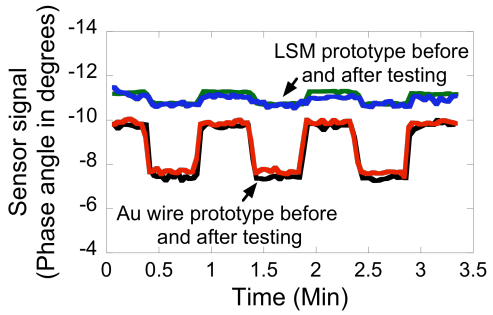

Figure 3. Sensing behavior of Au wire and LSM prototypes in 4% O_2 and 4% H_2O with 30 sec. pulses of 20 ppm NO prior to (black and green curves) and after (red and blue curves) being operated directly mounted into the exhaust manifold.

Evaluation on the Ford laboratory test stand after engine testing not only indicated improved sensor robustness, but was also used to investigate NH_3 cross-sensitivity. Figure 4 shows results of testing NH_3 cross-sensitivity in 10.5% O_2 and 4% H_2O with 30 sec. pulses of 50 ppm NO, 50 ppm NH_3, or 50 ppm of both NO and NH_3. The gas flow profile sequence is identified in Fig. 4a. In Fig. 4b, the response of the Au wire prototype (shown by the black curve) had higher sensitivity to NH_3 than NO, where only NH_3 was measured when both NO and NH_3 were added. In Fig. 4b, and in more detail in Fig. 4c, the response of the LSM prototype (shown by the green curve) had higher sensitivity to NO than NH_3, with more selectivity to NO when both were added.

The results on the Ford laboratory test stand were used to explain the results from the dynamometer engine testing. In all cases, engine testing resulted in the generation of less than a few ppm of NO_2; therefore, only NO concentrations are shown. Figure 5a and 5b show engine test results for the LSM and Au wire prototypes, respectively, where the red curve indicates the sensor response and corresponds to values on the left axis. The blue curve indicates the commercial NO_x sensor tested alongside in the manifold and corresponds to values on the right axis. The green curve indicates the NO concentration from gas analysis (FTIR) and also corresponds to values on the right axis.

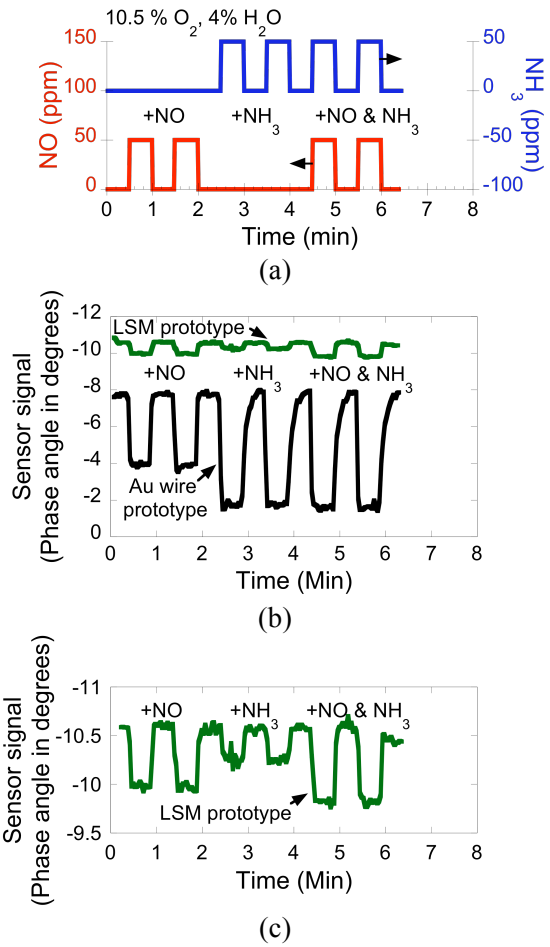

Figure 4. (a) Gas flow profile used for testing NH_3 cross-sensitivity with 30 sec. pulses of 50 ppm NO, 50 ppm NH_3, or 50 ppm of both NO and NH_3. (b) Measured response of Au wire and LSM prototypes and (c) expanded data for LSM prototype showing more detail.

The response of the LSM prototype in Fig. 5a had good correlation with both the commercial sensor and the gas analysis. The bottom of Fig. 5a also shows the measurement of NH_3 concentration from the gas analysis (the green curve corresponding to values on the right axis). In the bottom of Fig. 5a, from about 23 to 30 min., the NH_3 concentration increases from about 10 to 30 ppm with no change in the NO concentration. The commercial sensor, shown by the blue curve at the top of Fig. 5a, also increased from 23 to 30 min and indicated cross-sensitivity to NH_3. In contrast, the LSM prototype did not seem affected by changes in NH_3, with the response remaining flat from 23 to 30 min.

The response of the Au wire prototype in Fig. 5b did not correlate as well as the LSM prototype did with the commercial sensor and the gas analysis. Furthermore, the commercial sensor in the top of Fig. 5b (blue curve) also did not correlate well with the gas analysis (green curve). The behavior can be explained by the measured NH_3 concentration shown in the bottom of Fig. 5b by the green curve. High levels of NH_3, from 20 to 75 ppm, were measured. In Fig. 5b, both the Au wire prototype and commercial sensor detected changes in NH_3 concentration, including the spike in concentration at 20 to 23 min. Additionally, the Au wire prototype showed more selectivity to NH_3 than to NO, with the sensor response (red curve in bottom of Fig. 5b) correlating with the NH_3 concentration from gas analysis (green curve) instead of changes in the NO concentration (green curve in top of Fig. 5b).

The composition of real diesel exhaust was influenced by the history and age of the engine and exhaust after-treatment system. Testing revealed that the dynamometer engine test stand had significant "slip" where the exhaust after-treatment was unable to catalyze the NO_x reactions resulting in larger amounts of unreacted NH_3. Vehicle testing with better quality exhaust systems are planned that should yield lower levels of both NO and NH_3.

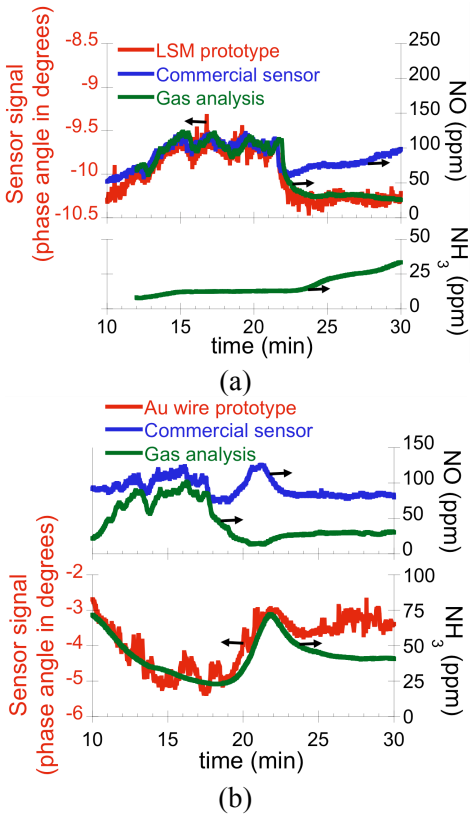

Figure 5. Engine dynamometer testing of (a) LSM and (b) Au wire prototypes mounted directly into exhaust manifold.

Au wire prototype: Strategy for improving accuracy using numerical algorithms

A more extensive study of the cross-sensitivity of the Au wire prototype was performed using a sensor fabricated on an alumina substrate (10 mm × 10 mm × 0.5 mm) without imbedded heaters. The alternative sensor design was more suitable for controlled temperature testing in a tube furnace. The sensor geometry was similar to that shown in Fig. 2a. The major noise factors were investigated which included temperature, water, and oxygen.

Before beginning the cross-sensitivity evaluation, the Au wire prototype was initially aged at 650°C for 720 hrs under dry conditions and demonstrated stable and reproducible response. The prototype was then aged at 650°C for 96 hrs in about 2% H_2O before beginning the evaluation.

Figure 6 shows the sensing behavior of the Au wire prototype design (top red curve) while the bottom blue curve shows the corresponding changes in the water concentration measured during testing. The response of the prototype for different oxygen and ppm NO concentrations was not influenced by spikes in the water concentration of about 2 to 4% indicating low water cross-sensitivity. Gas flow profiles stepped through 2, 10.5 and 18.9% O_2, with changes in NO concentration at each oxygen level (100, 50, 20, 10 ppm). The gas flow profile was used at three water concentrations (2, 4 and 6%) and three temperatures (625, 650, and 675°C). Measurements indicated water cross-sensitivity was minimized for operation at the intermediate temperature of 650°C.

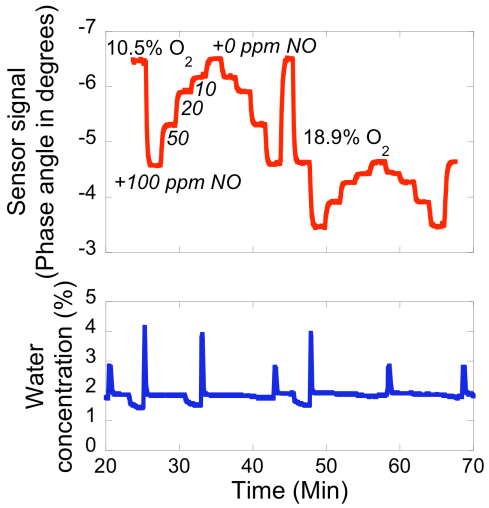

Figure 6. Sensing behavior of Au wire prototype (red curve) on an alumina substrate at 625°C in varying O_2 and NO concentrations, with corresponding changes in H_2O concentration (blue curve).

The data collected for the cross-sensitivity evaluation was used to develop a mathematical procedure for minimizing interferences, which can be summarized in three general steps. The first step is choosing an operating temperature to minimize water interference, which was found to be 650°C. The temperature can be assumed to be controlled to approximately ±5°C, and measurable to within 1°C.

The oxygen signal can be obtained using a separate measurement at a different frequency, as described in more detail in last year's report as well as in a previous publication.[8] At 1 kHz and T = 650°C, the prototype does not respond to NO and only responds to oxygen, allowing an independent measurement of the oxygen concentration. Figure 7 shows how the sensor signal at 1 kHz (θ_{1kHz}) varies with oxygen concentration ($\%O_2$). In Fig. 7, a linear curve fit (dotted line) is shown and given by the following equation:

$$\%O_2 = \frac{\theta_{1kHz} + 6.08}{0.0305} \qquad (1)$$

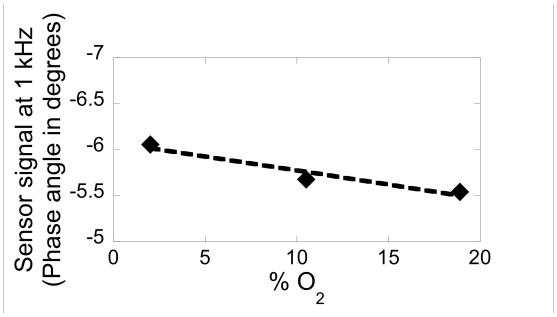

Figure 7. Measured sensor signal at 1 kHz (θ_{1kHz}) for different O_2 concentrations, with linear curve fit (dotted line).

Using both the measured temperature and oxygen, the second step then involves using additional numerical relationships, derived from fitting the data collected in the cross-sensitivity evaluation, to calculate the expected sensor signal for zero NO_x, or when NO_x is not present at the known temperature and oxygen level.

Figure 8a shows how the sensor signal (θ_{O2}) changes with oxygen concentration at 650°C when NO_x is not present, and the corresponding polynomial fit (dotted line) is given by the following equation:

$$\theta_{O2} = -14 + 1.2(\%O_2) - 0.035(\%O_2)^2 \qquad (2)$$

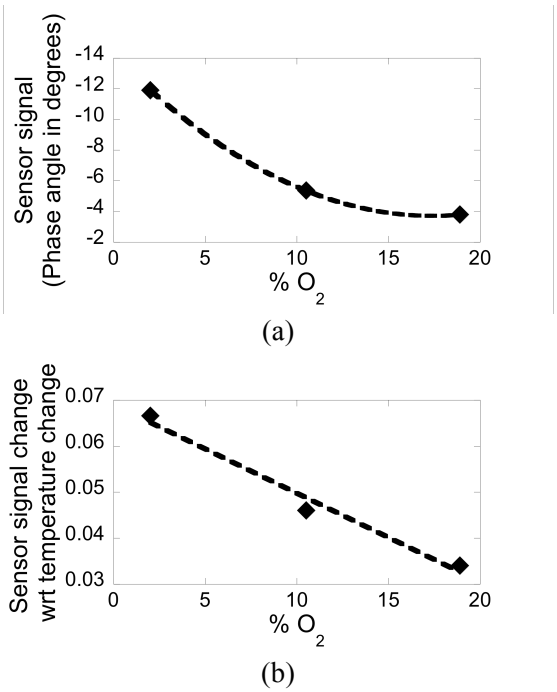

Figure 8. Influence of $\%O_2$ at 650°C when NO_x is not present on the (a) sensor signal (θ_{O2}), and on the (b) sensor signal with respect to (wrt) changes in temperature ($\Delta\theta/\Delta T$). Curve fits are shown as dotted lines.

Figure 8b shows how changes in the sensor signal with respect to changes in temperature ($\Delta\theta/\Delta T$) are influenced by oxygen concentration at 650°C when NO_x is not present, and the corresponding linear fit (dotted line) is given by the following equation:

$$\left(\frac{\Delta\theta}{\Delta T}\right)_{O2} = 0.069 - 0.0019(\%O_2) \quad (3)$$

The two values calculated by the relationships in Fig. 8a and 8b (Eqs. 2 and 3) and the measured temperature ($T_{measured}$) are then used to calculate the zero NO_x (θ_{ONOx}) using the following equations:

$$\theta_{0NOx} = \theta_{O2} + \left(\frac{\Delta\theta}{\Delta T}\right)_{O2} \Delta T \quad (4)$$

$$\Delta T = T_{measured} - 650 \quad (5)$$

Finally, in the third step, the difference between the calculated zero NO_x signal (θ_{ONOx}) and the actual measured NO_x signal ($\theta_{measured}$) is used to provide a measurement of the amount of NO_x that minimizes the influence of oxygen, water, and temperature.

Figure 9 shows how changes in the sensor signal with respect to changes in ppm NO ($\Delta\theta/\Delta NO$) are influenced by oxygen concentration at 650°C, and the corresponding polynomial fit (dotted line) is given by the following equation:

$$\left(\frac{\Delta\theta}{\Delta NO}\right)_{O2} = 0.055 - 0.0050(\%O_2) + 0.00014(\%O_2)^2 \quad (6)$$

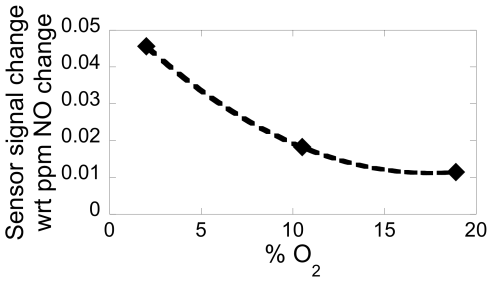

Figure 9. Influence of $\%O_2$ at 650°C on the sensor signal with respect to (wrt) changes in ppm NO ($\Delta\theta/\Delta NO$) and the corresponding best fit (dotted line).

The value calculated by the relationship in Fig. 9 (Eq. 6) is then used to determine the amount of measured NO_x (ΔNO), where the influence of fluctuations in oxygen, water, and temperature are now minimized, using the following equations:

$$\Delta NO = \frac{\Delta\theta}{\left(\frac{\Delta\theta}{\Delta NO}\right)_{O2}} \quad (7)$$

$$\Delta\theta = \theta_{0NOx} - \theta_{measured} \quad (8)$$

The cross-sensitivity relationships were also used to provide a rough estimate of sensor accuracy in terms of error or noise introduced by either temperature or water fluctuations. Since the measured sensor signal had a linear dependence on changes in both temperature and water concentration, changes in the sensor signal with respect to changes in ppm NO could be determined for changes in either temperature or water. The noise introduced varied with oxygen concentration, where the minimum noise occurred at 2% O_2. For oxygen concentrations ranging from 2 to 18.9%, noise from ± 1°C temperature fluctuations decreased NO accuracy by ~1.5 to 3 ppm NO, and noise from ±1% H_2O fluctuations de-

creased NO accuracy by ~1.2 to 2.2 ppm NO. The noise values need further improvement to meet the desired ±1 ppm, but are beginning to approach the accuracy required to meet emission limits.

Conclusions

Work in FY2010 included improving sensor robustness to allow testing of prototypes directly mounted onto the exhaust manifold. Previous attempts had required exhaust gases to be routed into a separate furnace for testing due to mechanical failure from engine vibrations. Real engine conditions caused either the Au wire or dense LSM to detach from the substrate. The modification of sensor prototypes by adding a ceramic adhesive successfully improved mechanical stability and robustness while simultaneously retaining the sensing performance.

Laboratory ammonia (NH_3) testing and engine dynamometer testing in real diesel exhaust were consistent with each other and found different behavior for the Au wire and LSM prototypes. The LSM prototype was found to be more selective than the Au wire prototype for NO when both NH_3 and NO were present.

Finally, a more extensive cross-sensitivity study was undertaken to examine major noise factors including fluctuations in water, oxygen, and temperature. The quantitative data were then used to develop a strategy using numerical algorithms to improve sensor accuracy. For oxygen concentrations ranging from 2 to 18.9%, noise from ± 1°C temperature fluctuations decreased NO accuracy by ~1.5 to 3 ppm NO, and noise from ±1% H_2O fluctuations decreased NO accuracy by ~1.2 to 2.2 ppm NO.

References

1. N. Yamazoe, *Sens. Actuators, B*, **108**, 2 (2005).
2. R. Moos, *Int. J. Appl. Ceram. Technol.*, **2**, 401 (2005).
3. S. Akbar, P. Dutta, and C. Lee, *Int. J. Appl. Ceram. Technol.*, **3**, 302 (2006).
4. F. Menil, V. Coillard, and C. Lucat, *Sensors and Actuators B,* **67**, 1 (2000).
5. S. Zhuiykov and N. Miura, *Sens. Actuators, B*, **121**, 639 (2007).
6. J. W. Fergus, *Sens. Actuators, B*, **121**, 652 (2007).
7. S. -W. Song, L. P. Martin, R. S. Glass, E. P. Murray, J. H. Visser, R. E. Soltis, R. F. Novak, and D. J. Kubinski, *J. Electrochem. Soc.*, **153**, H171 (2006).
8. L. P. Martin, L. Y. Woo, and R. S. Glass, *J. Electrochem. Soc.,* **154**, J97 (2007).
9. L. Y. Woo, L. P. Martin, R. S. Glass, and R. J. Gorte *J. Electrochem. Soc.,* **154**, J129 (2007).
10. L. Y. Woo, L. P. Martin, R. S. Glass, W. Wang, S. Jung, R. J. Gorte, E. P. Murray, R. F. Novak, and J. H. Visser. *J. Electrochem. Soc.,* **155**, J32 (2008).
11. L.Y. Woo, R.S. Glass, R.F. Novak, and J.H. Visser. *J. Electrochem. Soc.*, **157**, J81 (2010).

Publications/Presentations

L.Y. Woo, R.S. Glass, R.F. Novak, and J.H. Visser. "Effect of electrode material and design on sensitivity and selectivity for high temperature impedancemetric NO_x sensors." *J. Electrochem. Soc.*, 157(3):J81-87, 2010.

Oral presentation entitled "Impedancemetric NO_x Gas Sensors Based on Porous YSZ for Diesel Exhaust: O_2 and Water Cross-Sensitivity" at The American Ceramic Society 34th International Conference and Exposition on Advanced Ceramics and Composites, in Daytona Beach, Florida, January 24-29, 2010.

Oral presentation entitled "Long-Term and Temperature Cycling Stability of Impedancemetric NO_x Gas Sensors Based On Porous Yttria-Stabilized Zirconia (YSZ)" at the 217th Meeting of the Electrochemical Society, in Vancouver, British Columbia, Canada, April 26-30, 2010.

Oral project presentation at the 2010 DOE Vehicle Technologies and Hydrogen Programs Annual Merit Review and Peer Evaluation Meeting, June 7-11, 2010 in Washington, D.C.